The viscosity-average molecular weight was estimated from intrinsic viscosities in 0.002 M HCl solution.[17] Unless otherwise specified, the sample with $\bar{M}_v = 2.3 \times 10^5$ was used. Auramine O was recrystallized from hot methanol and melted at 265–267 °C (lit[18] 267 °C).

Solutions of PMA were prepared with deionized water. The concentration was determined by titration with 0.1 N NaOH in the presence of 0.3 M NaCl. Since AO decomposes slowly, a stock solution was prepared once a week and stored at low temperature in the dark. Potassium phthalate buffers were used for pH 4 and 5, phosphate buffers for pH 6, 7, and 8.

Absorption spectra were recorded on a Cary 2300 UV spectrometer. A Perkin-Elmer MPF-44B fluorescence spectrophotometer was used for static fluorescence measurements. Kinetic fluorescence measurements were carried out on the instrument used in a previous study.[9] Results of at least 10 runs were averaged by the computer to minimize noise rate constants with the best fit to the data were computed.

Acknowledgment. We are grateful for the support of this study by Grant DMR 85-00712, Polymers Program, of the National Science Foundation.

Registry No. AO, 2465-27-2; PMA, 25087-26-7.

References and Notes

(1) Oster, G. *C. R. Hebd. Séances Acad. Sci. 1951, 232,* 1708.
(2) Oster, G. *J. Polym. Sci.* **1955**, *16*, 235.
(3) Oster, G.; Nishijima, Y. *J. Am. Chem. Soc.* **1956**, *78*, 1581.
(4) Leyte, J. C.; Mandel, M. *J. Polym. Sci., Part A.* **1964**, *2*, 1879.
(5) Anufrieva, E. V.; Birshtein, T. M.; Nekrasova, T. N.; Ptitsyn, O. B.; Sheveleva, T. V. *J. Polym. Sci., Part C* **1968**, *C16*, 3519.
(6) Stork, W. H. J.; Van Boxsel, J. A. M.; De Goeij, A. F. P. M.; De Haseth, P. L.; Mandel, M. *Biophys. Chem.* **1974**, *2*, 127.
(7) Chen, T. S.; Thomas, J. K. *J. Polym. Sci., Polym. Chem. Ed.* **1979**, *17*, 1103.
(8) Bednář, B.; Morawetz, H.; Shafer, J. A. *Macromolecules* **1984**, *17*, 1634.
(9) Bednář, B.; Morawetz, H.; Shafer, J. A. *Macromolecules* **1985**, *18*, 1940.
(10) Muller, G.; Fenyo, J. C. *J. Polym. Sci., Polym. Chem. Ed.* **1978**, *16*, 77.
(11) Schubert, W. M.; Craven, J. M. *J. Am. Chem. Soc.* **1960**, *82*, 1357.
(12) Erny, B.; Muller, G. *J. Polym. Sci., Polym. Chem. Ed.* **1979**, *17*, 4011.
(13) Braud, C. *Eur. Polym. J.* **1977**, *13*, 897, 901.
(14) Fenyo, J. C.; Magnol, L.; Delben, F.; Paoletti, S.; Crescenzi, V. *J. Polym. Sci., Polym. Chem. Ed.* **1979**, *17*, 4069.
(15) Mandel, M.; Stork, W. H. J. *Biophys. Chem.* **1974**, *2*, 137.
(16) Kenner, R. A.; Aboderin, A. A. *Biochemistry* **1971**, *10*, 4433.
(17) Katchalsky, A.; Eisenberg, H. *J. Polym. Sci.* **1951**, *6*, 145.
(18) Graebe, G. *Ber.* **1887**, *20*, 3260.

Electron Spin Resonance Study of the Photooxidation Mechanism in Poly(*n*-butyl acrylate): Photochemical Processes in Polymeric Systems. 11

Soon Sam Kim,* Ranty H. Liang, Fun-Dow Tsay, and Amitava Gupta*

Applied Sciences and Microgravity Experiments Section, Jet Propulsion Laboratory, California Institute of Technology, Pasadena, California 91109.
Received December 10, 1985

ABSTRACT: Kinetics of the reactions of the principal radical species, the tertiary alkyl and peroxy radicals, generated on photooxidation of poly(*n*-butyl acrylate) (PnBA) were studied at room temperature under different oxygen pressures. A simplified mechanism of photooxidation, similar to that proposed earlier (Liang, R. H.; Tsay, F.-D.; Gupta, A. *Macromolecules* **1982**, *15*, 974), was used to interpret the data. The kinetic rate parameters as well as the radical concentrations developed under steady-state illumination conditions were estimated by a least-squares fit to the observed data by using kinetic equations based on such a mechanism. It was found that at least two different types of tertiary alkyl radicals (i.e., radicals of different reactivities) were being formed during photooxidation of PnBA.

Introduction

Details of the mechanism of photooxidation of polymers are becoming increasingly clearer mainly through the efforts of Scott,[2-4] Guillet,[5,6] and others.[7-9] Generally speaking, this mechanism involves the participation of the polymeric tertiary alkyl radicals and the peroxy radicals formed by reaction of the tertiary alkyl radicals with oxygen as shown in Scheme I. In our earlier study on the photodegradation of PnBA,[1] we showed that the primary radicals formed at initial photolysis underwent a series of abstraction and rearrangement processes until at room temperature the only surviving radical in the system was a polymeric tertiary alkyl radical in the absence of oxygen. Under high oxygen pressures (≥150 torr), the only detectable species was a macromolecular peroxy radical. We therefore planned a brief series of time-resolved UV (broad band, $\lambda \geq 250$ nm) photooxidation studies in order to obtain the yield and kinetics of these radical species. The results reported below show that even in its simplest form the photooxidation mechanism is more complex than is indicated by the simple mechanism shown in Scheme I; in particular, the mechanism is found to involve at least

Scheme I

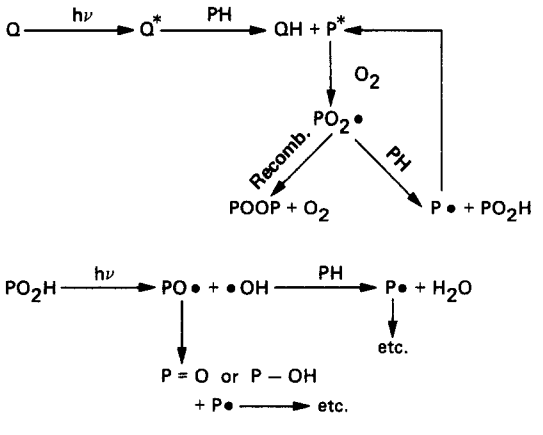

two different types of metastable tertiary alkyl radicals of significantly different reactivities.

Since its glass transition temperature is 210 K, at room temperature PnBA in the solid state manifests high permeability to oxygen molecules. The resulting photo-

0024-9297/86/2219-1930$01.50/0

chemistry is therefore sensitive to the ambient oxygen concentration, particularly at low oxygen partial pressures. For example, the equilibrium between tertiary alkyl and peroxy radicals depends on the availability of oxygen in the irradiated films. For these reasons the kinetics were studied at several oxygen pressures with thin films of PnBA.

Experimental Section

Sample Preparation. Poly(*n*-butyl acrylate) was synthesized via thermal polymerization by refluxing the monomer in cyclohexane under nitrogen. The polymer was purified by dissolving the sample in dichloromethane and then reprecipitating it by adding methanol to the dichloromethane solution.

Samples for ESR experiments were prepared as follows: the polymer sample was redissolved in dichloromethane, and the solution was pipetted into quartz ESR sample tubes (3 mm i.d., 4 mm o.d., and 10 cm long) with ground joints. The ESR tubes with polymer solution were then connected to a vacuum line and pumped overnight. Usually a thin film (≈5 μm) of PnBA (≈25 mg) was formed inside the sample tubes. After pumping, oxygen was introduced into the tubes at known partial pressures, e.g., 1, 10, 50, and 760 torr. The tubes were then sealed off with a torch.

ESR Experiments. For the photochemical studies, the PnBA sample was placed inside an ESR microwave cavity (Varian, Century series, E-115) equipped with a grid opening for light irradiation. An UV-enhanced xenon lamp (ILC Technology, LX300UV) was used as a light source. Light from the lamp was filtered through a water filter (4-cm path length) and focused onto the sample inside the cavity by a quartz lens. The spectral distribution of the lamp is known to extend down to 250 nm.

For kinetic studies, the magnetic field of the ESR spectrometer was fixed at one of the peak positions of the radical spectrum, and the light was modulated (on and off) at programmed time intervals through an electronic shutter (Ealing). During each irradiation period, a rise period, a period of steady-state illumination (during which radical populations remained constant), and a period of radical decay could be monitored.

A trigger source (HP 3310A function generator) was used to synchronize a signal averager (EG&G PAR 4203) and the shutter. Typical repetition rate of the trigger source for signal averaging was 0.004 Hz (period of 250 s).

For each kinetic study, a fresh PnBA sample was used, and only the initial five scan averages were collected to minimize the effect of aging of the samples which would alter the kinetics of radical reactions. All the ESR data were obtained at a microwave power of 5 mW. The data were checked for saturation effects by varying the power from 0.05 to 100 mW. No sign of saturation was observed at 5 mW.

Concentrations of radical species were estimated by comparing areas under ESR absorption spectra with the area of Tanol standard. The areas were obtained after double integration of derivative ESR spectra by using a Varian supplied software.

Heating and cooling of samples were effected by blowing hot or cold nitrogen gas through a Dewar assembly held inside the ESR cavity. The sample temperature was maintained at a specified value through a temperature controller unit (Varian V4540).

Results

In the previous study of PnBA,[1] radical species were generated at 77 K through irradiation from a laser (266 nm) source. They were studied by ESR at several temperatures ranging from 77 to 213 K. In this study, the PnBA film was irradiated in situ inside the ESR microwave cavity at room temperature, and the kinetics of the radical species generated were studied under different oxygen pressures. Quantum yields of radical formation could not be estimated because of the uncertainties involved in estimation of the total number of photons absorbed by the polymer film.

Assignments. When irradiated with UV light at room temperature, the PnBA film under vacuum showed a triplet ESR spectrum (g = 2.0023, hyperfine coupling constant 24.6 G, with peak intensity ratio, 1:2:1), which was assigned to the main-chain tertiary alkyl radical species, $-CH_2\dot{C}(COOC_4H_9)CH_2-$[1,10] (see Figure 1). As oxygen was introduced into the sample, the ESR spectrum gradually changed to a broad single peak (g = 2.014, line width 14.0 G). This peak was assigned to peroxy radicals, $-CH_2CH(OO\bullet)CH_2-$[1] and $-CH_2COO\bullet(COOC_4H_9)CH_2-$.

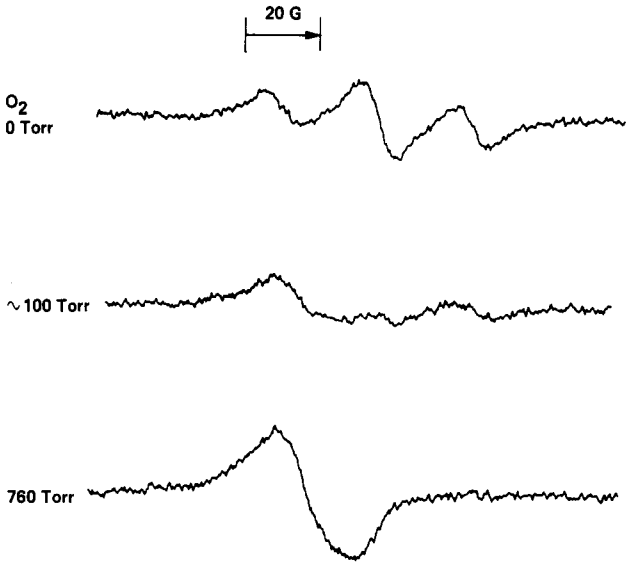

Figure 1. ESR spectra of photogenerated radicals from PnBA film under different O_2 pressures.

In order to confirm the above assignments, the radical species were studied at different temperatures. The PnBA sample under vacuum was heated in the microwave cavity, and the resulting ESR spectra during UV illumination were recorded at 22, 55, 75, and 100 °C (see Figure 2). As heating progressed, the outer peaks of the triplet began to show hints of splitting at 55 °C. At 75 °C, they split in two with hyperfine coupling constants of 28.5 and 21.1 G, respectively.

It is reported earlier[10-15] that the four hydrogen atoms in tertiary alkyl radicals are not equivalent because of their limited motions in the polymer matrix. It seems from the heating experiments, the room temperature triplets are from two unresolved sets of slightly inequivalent β protons, H_1 and H_2, each with intensity ratios of 1:2:1. (see Figure 3). When heated, thermal motion around the equilibrium position narrows the spectral line width and resolves the splittings of two inequivalent protons. From the theory of hyperconjugation[16] the proton splittings can be expressed approximately as

$$a_{\beta H} = B \cos^2 \theta \qquad (1)$$

in which θ is an angle of twist between the α-carbon $2p_z$ orbital and the plane containing the β-proton C–H bond. (see Figure 3). The angles, θ_1 and θ_2 for protons H_1 and H_2, can be estimated by using eq 1. With the constant B set at a typical methyl proton value of 46 G,[14] the estimated angles, θ_1 and θ_2, are 38 and −47°, respectively.

In order to check the effect of butyl side chains on the observed ESR spectra, a sample of poly(isobutyl acrylate) was tested under UV irradiation. The results are shown in Figure 4. At the beginning of irradiation, the sample showed an extra peak (26.8 G line width) overlapped with the familiar triplet ESR spectrum observed from PnBA films. However, as the UV irradiation continued, intensity of the extra peak decreased and the triplet structure persisted. From this observation, one can deduce that the spectrum with triplet structure is from main-chain alkyl radicals, and they are not directly affected by the side-

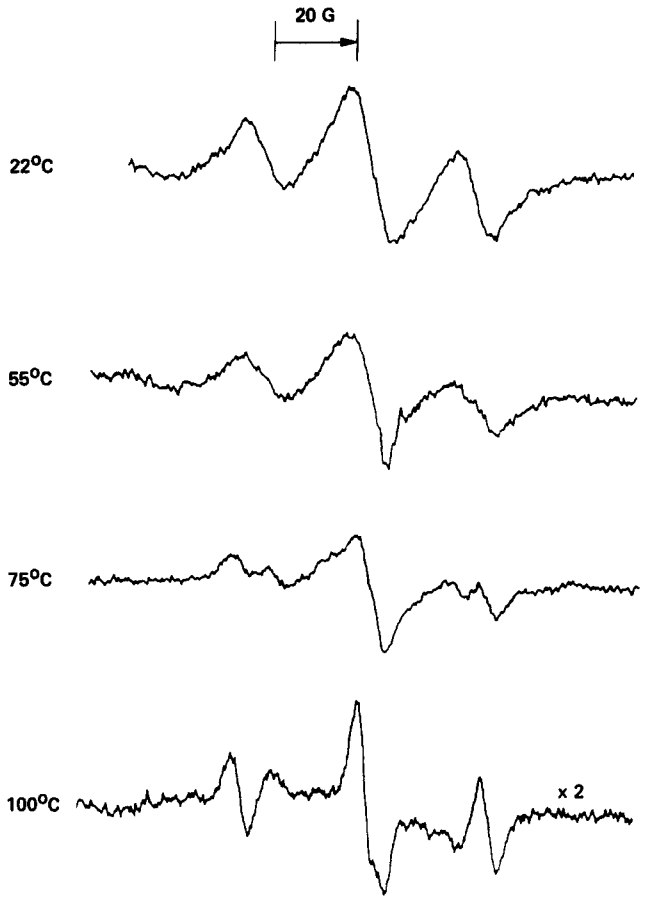

Figure 2. ESR spectra of tertiary alkyl radicals as a function of temperature. The PnBA film was under vacuum.

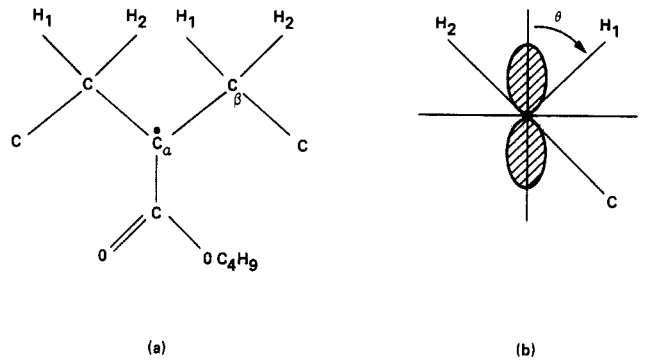

Figure 3. (a) Model for a tertiary alkyl radical. (b) Projection in a plane perpendicular to the α and β carbon C–C bond.

chain configurations. The nature of the extra peak was not persued in this study.

The single peak observed from the PnBA sample under oxygen was studied further at lower temperatures. The samples were cooled in situ inside the ESR cavity to the specified temperatures, −12, −40, and −70 °C, and irradiated by UV light. The spectrum at 77 K was obtained as follows: the sample was first cooled to ≈150 K and irradiated by UV light for ≈2 min. The sample was then quickly cooled to 77 K by plunging the tube into a Dewar containing liquid N_2. The results are shown in Figure 5. As the temperature is lowered, the spectrum broadens and finally splits into two components at 77 K. This is a typical peroxy spectrum observed in earlier studies.[1]

At 77 K, the molecular motions of the polymer network are practically frozen, and the observed spectrum shows anisotropic g-tensor splittings (g_1, g_2, and g_3) of peroxy radicals. However, as the temperature is raised from 77 K, the g-tensor anisotropy is averaged over molecular

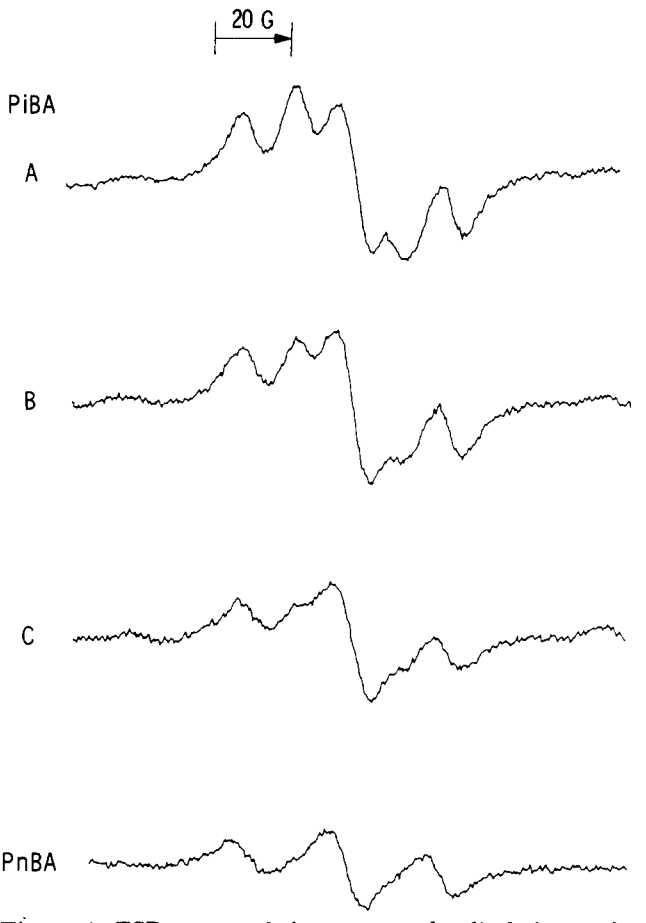

Figure 4. ESR spectra of photogenerated radicals from poly(isobutyl acrylate) at room temperature: (A) at the beginning of UV irradiation; (B) after ≈10 min of irradiation; (C) after ≈20 min of irradiation. The tertiary alkyl radical spectrum from PnBA film is shown for comparison.

motions, and the splitting gradually coalesces to a single peak at room temperature. Similar observations were reported by several authors.[17,18]

Kinetics. The rise and decay kinetics of the photogenerated radicals have been measured at room temperature under different oxygen pressures. The results are shown in Figures 6 and 7. As shown in Figure 1, at intermediate oxygen pressures the observed ESR spectra consist of an overlap of spectra of tertiary alkyl and peroxy radicals. In monitoring the tertiary alkyl radical kinetics, the highest field peak (indicated by an arrow in Figure 6) of the triplet spectrum was used in order to minimize the contribution from the peroxy radicals. The kinetics of peroxy radicals were measured at 760 torr of oxygen pressure, where the ESR spectrum is overwhelmingly from the peroxy radicals (see Figure 7).

In the previous study performed at lower temperatures,[1] many radical species were observed, e.g., $-CH_2CH(CO\bullet)-CH_2-$, $-CH_2CH(COO\bullet)CH_2-$, $-CH_2\dot{C}HCH_2-$, and $\bullet CHO$. On the basis of these observations, a mechanistic model of the photochemical processes in the PnBA matrix was presented (Schemes I and II in ref 1). However, at room temperature the stable radicals under UV irradiation are the tertiary alkyl radicals (under vacuum) or peroxy radicals (under air). All other radicals mentioned above became short-lived at this temperature and could not be detected by ESR.

In the kinetic modeling to simulate the observed rise and decay curves shown in Figures 6 and 7, it was necessary to simplify the mechanistic model presented in ref 1; e.g., all the short-lived intermediate radicals at room temper-

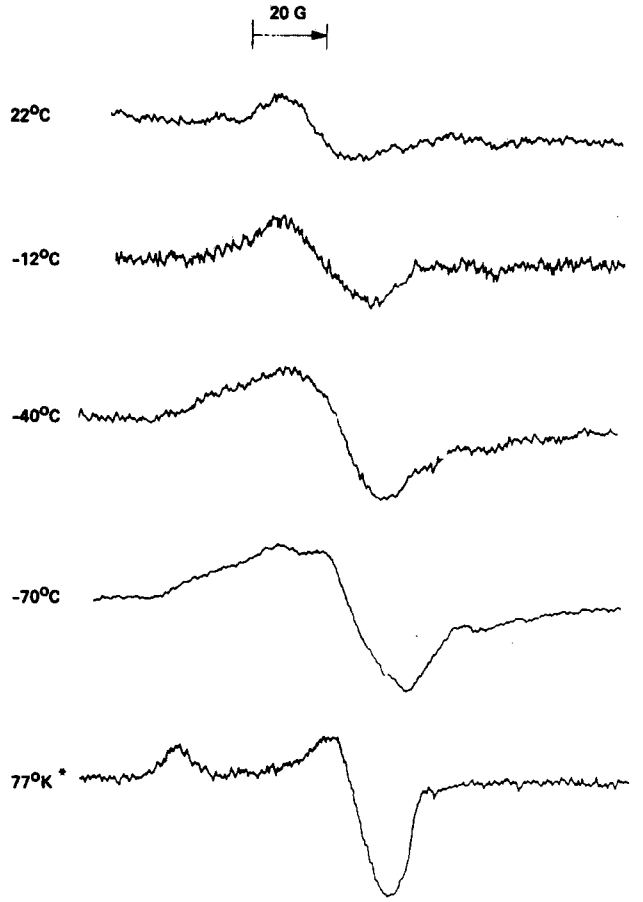

Figure 5. ESR spectra of peroxy radicals as a function of temperature. The spectrum at 77 K was obtained by first irradiating the film at 150 K and then cooling to 77 K.

Scheme II

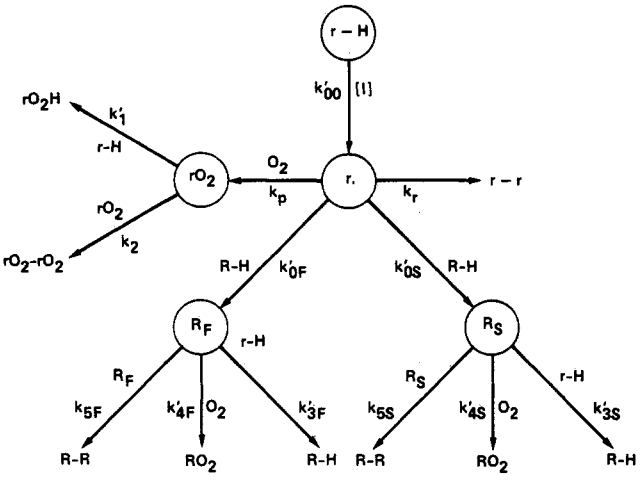

ature were represented as radical "r".

The resulting photooxidation scheme, shown as Scheme II, postulates two different tertiary alkyl radicals, R_F and R_S, needed to simulate the rise and decay curves using a unique set of kinetic parameters. It is possible that tertiary alkyl radicals of different mobilities and chain lengths are involved, and the proposed representative in Scheme II is an approximate and simplified picture which will allow an acceptable fit to the data. It also shows that the peroxy radicals are formed directly from the intermediate short-lived radicals as well as on reaction of oxygen with the tertiary alkyl radicals.

The fitting procedure was also attempted with a simpler scheme, i.e., with only one type of tertiary alkyl radicals; however, no reasonable fitting could be achieved.

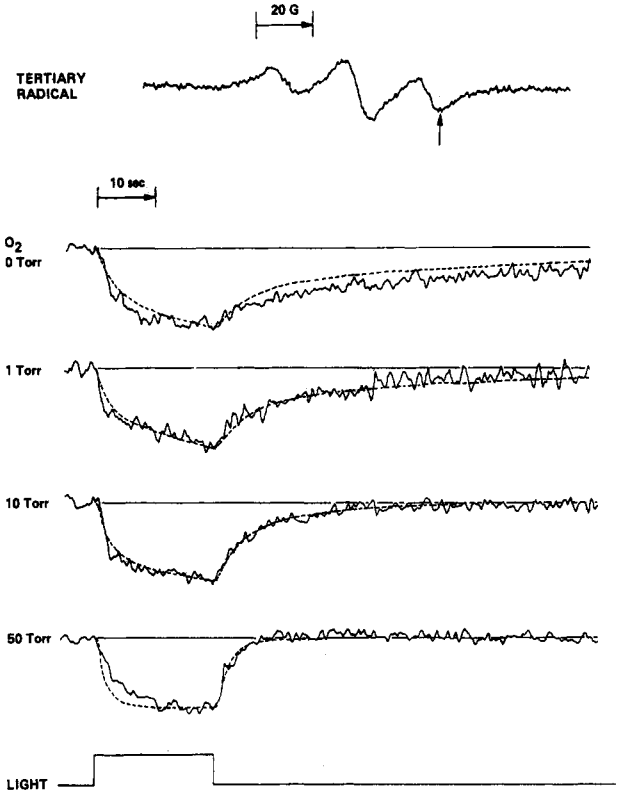

Figure 6. Rise and decay characteristics of tertiary alkyl radicals at room temperature as a function of O_2 pressure. The radical signal intensity was monitored at the peak indicated by an arrow. The experimentally observed curves (solid line) are overlapped with calculated ones (broken line).

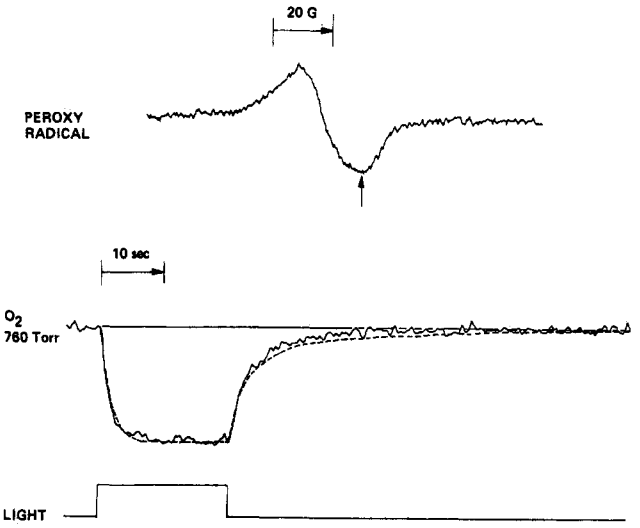

Figure 7. Rise and decay characteristics of peroxy radicals at room temperature. The experimentally observed curve (solid line) is overlapped with a calculated one (broken line).

According to the kinetic model shown in Scheme II, one can set up the following differential equations:

intermediate radical: r

$$d[r]/dt = k'_{00}[I] - \{k'_{0F} + k'_{0S} + k_p[O_2]\}[r] - k_r[r]^2 \quad (2)$$

in which [I] = intensity of light

tertiary radical: R_F and R_S

$$d[R_F]/dt = k'_{0F}[r] - \{k'_{3F} + k'_{4F}[O_2]\}[R_F] - k_{5F}[R_F]^2 \quad (3)$$

$$d[R_S]/dt = k'_{0S}[r] - \{k'_{3S} + k'_{4S}[O_2]\}[R_S] - k_{5S}[R_S]^2 \quad (4)$$

peroxy radical: rO_2

$$d[rO_2]/dt = k_p[O_2][r] - k'_1[rO_2] - k_2[rO_2]^2 \quad (5)$$

Table I
Best-Fit Kinetic Parameters for Scheme II

radical	steady-state population	rate process	rate constants (25 °C)
intermediate	$[r]_{eq} = 2.4 \times 10^{-6}$ mol/L	reaction with O_2	$k_p = 700$ L mol^{-1} s^{-1}
		recombination	$k_r = 8 \times 10^5$ L mol^{-1} s^{-1}
tertiary	$[R_F]_{eq} = 4.4 \times 10^{-6}$ mol/L	formation of R_F	$k'_{0F} = 5 \times 10^{-1}$ s^{-1}
	$[R_S]_{eq} = 2.9 \times 10^{-6}$ mol/L	formation of R_S	$k'_{0S} = 1 \times 10^{-1}$ s^{-1}
		abstraction by R_F	$k'_{3F} = 1.3 \times 10^{-1}$ s^{-1}
		abstraction by R_S	$k'_{3S} = 8 \times 10^{-3}$ s^{-1}
		R_F reaction with O_2	$k'_{4F} = 700$ L mol^{-1} s^{-1}
		R_S reaction with O_2	$k'_{4S} = 300$ L mol^{-1} s^{-1}
		R_F recombination with self	$k_{5F} = 5 \times 10^4$ L mol^{-1} s^{-1}
		R_S recombination with self	$k_{5S} = 3 \times 10^3$ L mol^{-1} s^{-1}
peroxy	$[rO_2 + RO_2]_{eq} = 8.0 \times 10^{-6}$ mol/L	abstraction	$k'_1 = 2 \times 10^{-2}$ s^{-1}
		recombination with self	$k_2 = 5 \times 10^4$ L mol^{-1} s^{-1}

The decay of tertiary alkyl radicals via formation of peroxy radicals (RO_2) in eq 3 and 4 was taken into account only for the tertiary alkyl kinetics. Since no steady-state peroxy radical was detected by ESR at O_2 pressures lower than 50 torr, contribution of this route to the formation of peroxy was neglected and not incorporated in eq 5.

As the oxygen pressure increases, the following inequality holds:

$$k_p[O_2] \geq k'_{0F} + k'_{0S} \quad (6)$$

and the major decay path for the intermediate radials, r, is to form peroxy radicals. Formation of tertiary radicals becomes unimportant.

The rate constants, k_i, were determined by least-squares fits to the observed radical concentration profiles shown in Figures 6 and 7. For the tertiary alkyl radical kinetics under 50 torr of O_2 pressure, eq 2–4, were used. For the peroxy radical at 760 torr of O_2 pressure, only eq 2 and 5 were used.

It is important to note that the same set of kinetic parameters were used to fit the generation and decay profiles of both tertiary alkyl and peroxy radicals at different oxygen pressures. Only the values of oxygen concentration, $[O_2]$, were variable in these simulations.

The $[O_2]$ values used in this fitting were the concentrations of O_2 dissolved in the PnBA matrix under equilibrium with the O_2 pressures introduced initially into the sample tubes. Mole ratio solubility of oxygen[19,20] in hydrocarbons, 0.002, for O_2 partial pressure of 1 atm at 25 °C was used in the calculation.

The value of $[O_2]$ was kept constant for each curve at the initial value under the assumption that the oxygen concentration in the film is larger compared with the radical concentration. This is a reasonable assumption except at low oxygen pressures, e.g., 1 torr. Typical tertiary alkyl radical concentration at equilibrium, $[R_F] + [R_S]$, is 7×10^{-6} mol/L, and the value of $[O_2]$ dissolved in the film under 1 torr is 2×10^{-5} mol/L.

The differential equations were solved numerically by a computer program package from IMSL library. The rate constants were searched by best fitting the calculated curves to the observed ones. The best rate constants are shown in Table I. In Figures 6 and 7, the curves calculated by using these constants (broken line) are compared with the observed ones (solid line).

Discussion

The intermediate radicals (r) in PnBA are formed on absorption of short-wavelength UV photons (250 nm < λ < 300 nm) and subsequent photolysis of the ester moieties. Some of the differences between Schemes I and II undoubtedly arise from this efficient radical generation pathway provided in our system. Others, such as the postulated existence of more than one type of tertiary alkyl radical, are probably a reflection of the effect of the details of the molecular structure of the polymer on the photooxidation pathway.

For all intermediate radicals taken together, a typical concentration at equilibrium, $[r]_{eq}$, when calculated by using the best-fit parameters (see Table I), is about $^1/_3$ of the corresponding value for the tertiary alkyl radical, $[R]_{eq}$. At oxygen pressures below 50 torr, the recombination rate of the intermediate radical, $k_r = 1.92$, is larger than the sum of the pseudo-first-order decay rates, i.e., $k'_{0F} + k'_{0S} + k_p[O_2] \leq 1.4$. At these pressures, the major decay route of the intermediate radicals is the recombination path. However, at higher O_2 pressures, e.g., 100 torr, the rate of formation of the peroxy radical becomes larger, $k_p[O_2] = 1.95$, and this becomes the major decay route for the intermediate radicals.

As shown in Figure 1, with the increase of oxygen pressure the formation of peroxy radical increased and the inequality of eq 6 was fulfilled at 50 torr of oxygen pressure. At higher than 50 torr, the formation of the peroxy radical dominates over that of the tertiary alkyl radical. At 760 torr, the formation rate of the peroxy radical is ≈20 times faster and its decay rate is ≈20 times slower than those of the tertiary alkyl radical, and hence only peroxy radicals are observed at steady state under these conditions.

The major decay route of tertiary alkyl radicals is pseudo first order (reaction with O_2) at O_2 pressures higher than 50 torr, and the recombination rate of the larger tertiary alkyl radicals, k_{5S}, is 10 times slower than that of the smaller radicals, k_{5F}.

For peroxy radicals at equilibrium, the pseudo-first-order abstraction rate, k'_1, is 20 times smaller than the value $k_2[rO_2]$ for the second-order decay due to recombination. The major decay route for the peroxy radicals thus seems to be the second-order recombination reaction between peroxy radicals, leading to cross-linking.[21]

The rate constants shown in Table I may be compared with data reported by Denisov.[22,23] He found the rate constant of macroalkyl radical recombination in polypropylene at 370 K to be 5×10^5 L mol^{-1} s^{-1}, whereas the corresponding rate constants we found in PnBA to be 5×10^4 L mol^{-1} s^{-1} (k_{5F}) and 3×10^3 L mol^{-1} s^{-1} (k_{5S}) at 298 K. He also provided rate constants for hydrogen abstraction by alkyl radicals in polypropylene. His value of 10^2 L mol^{-1} s^{-1} at 393 K should be compared with our value of 0.13 s^{-1} (k'_{3F}) and 0.5 s^{-1} (k'_{0F}) at 298 K. Guillet and Somersall[24] reported the rate of hydrogen abstraction by peroxy radicals in ethylene vinyl acetate (EVA) at 298 K to be 0.1×10^{-2} L mol^{-1} s^{-1}, whereas our value after adjustment for R–H concentration (8.4 M) was 0.2×10^{-2} L mol^{-1} s^{-1} in PnBA. They also found the rate of recombination of peroxy radicals in EVA to be 1×10^4 L mol^{-1} s^{-1},

whereas our value, k_2, was 5×10^4 L mol^{-1} s^{-1}. Chien and Boss[25] studied kinetics of autooxidation in polypropylene at 383 K and reported corresponding rate constants of peroxy radicals: for hydrogen abstraction, 1.9 L mol^{-1} s^{-1}, and recombination, 3×10^6 L mol^{-1} s^{-1}.

Conclusions

In conclusion, we have experimentally tested the applicability of the basic autocatalytic photooxidation mechanism to photooxidation of PnBA using ESR techniques. We find that while peroxy and tertiary alkyl radicals are the major radical intermediates as required by the currently accepted mechanism, there seem to be significant differences in the reaction kinetics of the major intermediates and the mechanism of their formation. The macromolecular peroxy radicals are formed through two separate pathways: oxidation of short-lived intermediate radicals and oxidation of tertiary alkyl radicals. There are at least two different types of tertiary alkyl radicals, one being significantly smaller (and more mobile) than the other. Under the illumination conditions provided in this study, cross-linking by recombination of peroxy radicals is the major degradation pathway, cross-linking of tertiary alkyl radicals becoming important only in oxygen-starved samples.

Acknowledgment. We thank Dr. Robert F. Fedors for many helpful discussions. This paper represents one phase of research performed at the Jet Propulsion Laboratory sponsored by the National Aeronautics and Space Administration under Contract NAS7-918. This research was performed in support of the Flat-Plate Solar Array Project, Reliability Encapsulation Task, sponsored by the Department of Energy.

Registry No. Poly(*n*-butyl acrylate) (homopolymer), 9003-49-0.

References and Notes

(1) Liang, R. H.; Tsay, F. D.; Gupta, A. *Macromolecules* **1982**, *15*, 974.
(2) Scott, G. *ACS Symp. Ser.* **1976**, *25*, 340.
(3) Chakraborty, K. B.; Scott, G. *Polymer* **1977**, *18*, 98.
(4) Ghaffar, A.; Scott, A.; Scott, G. *Eur. Polym. J.* **1977**, *13*, 89.
(5) Sitek, F.; Guillet, J. E. *J. Polym. Sci., Symp. Ser.* **1976**, *57*, 343.
(6) Somersall, A. C.; Guillet, J. E. *Polym. Prepr. (Am. Chem. Soc., Div. Polym. Chem.)* **1984**, *25*, 60.
(7) Bolland, J. L. *Q. Rev., Chem. Soc.* **1949**, *3*, 1.
(8) Carlsson, D. J.; Garton, A.; Wiles, D. M. In *Developments in Polymer Stabilization 1*; Scott, G., Ed.; Aplied Science: Barking, UK; 1979; p 219.
(9) Carlsson, D. J.; Wiles, D. M. *J. Macromol. Sci., Rev. Macromol. Chem.* **1976**, *C14*, 65.
(10) Szocs, F.; Rostasova, O. J. *J. Appl. Polym. Sci.* **1974**, *18*, 2529.
(11) Abraham, R. J.; Whiffen, D. H. *Trans. Faraday Soc.* **1958**, *54*, 1291.
(12) Lykos, P. G. *J. Chem. Phys.* **1960**, *32*, 625.
(13) Ogawa, S. *J. Phys. Soc. Jpn.* **1960**, *16*, 1488.
(14) Symons, M. C. R. *J. Chem. Soc.* **1963**, 1186.
(15) Fischer, H. *J. Polym. Sci., Part B* **1964**, *2*, 529.
(16) Carrington, A.; McLachlan, A. D. *Introduction to Magnetic Resonance*; Harper and Row: New York, 1967; pp 83–85.
(17) Moriuchi, S.; Nakamura, M.; Shimada, S.; Kashiwabara, H.; Sohma, J. *Polymer* **1970**, *11*, 630.
(18) Suryanarayana, D.; Kevan, L.; Schlick, S. *J. Am. Chem. Soc.* **1982**, *104*, 668.
(19) Gerrard, W. *Solubility of Gases and Liquids, A Graphic Approach*; Plenum: New York, 1976; p 73.
(20) One can convert the mole ratio solubility of oxygen, 0.002, into appropriate units of Henry coefficient for PnBA and obtain $\gamma = 2.22 \times 10^{-5}$ mol L^{-1} torr^{-1}. This value is in good agreement with the value cited by Denisov[22] for the case of petroleum.
(21) Dickinson, H. R.; Rogers, C. E.; Simha, R. "Polymers in Solar Energy Utilization"; ACS Symposium Series 220; American Chemical Society: Washington, DC, 1983; pp 275–292.
(22) Denisov, E. T. *Dev. Polym. Stab.* **1982**, *5*, 23.
(23) Denisov, E. T. *Vysokomol. Soedin., Ser. A* **1977**, *19*, 2513.
(24) Somersall, A. C.; Guillet, J. E. Annual Report, 1981, DOE/JPL-955591-82/1, "Modeling of Photodegradation in Solar Cell Modules of Substrate and Superstrate Design made with Ethylene-Vinyl Acetate as Pottant Material".
(25) Chien, J. C. W.; Boss, C. R. *J. Polym. Sci., Polym. Chem. Ed.* **1967**, *5*, 3091.

On Blends of Poly(vinylidene fluoride) and Poly(vinyl fluoride)

Gaetano Guerra,† Frank E. Karasz,* and William J. MacKnight

Polymer Science and Engineering Department, University of Massachusetts, Amherst, Massachusetts 01003. *Received March 17, 1986*

ABSTRACT: Experimental evidence indicating immiscibility of the homopolymers poly(vinylidene fluoride) and poly(vinyl fluoride), both in the crystalline and amorphous phases, is presented. The X-ray analysis of the blended samples reveals patterns that are relatively insensitive to blend composition and that are similar to those found in previous studies. However, corresponding differential scanning calorimetry scans show well-defined and separate melting peaks of the component homopolymers, indicating immiscibility in the crystalline phase. In addition, the dynamic mechanical analysis indicates that the main relaxations of the two pure homopolymers are still present in the blend spectrum, implying also an immiscibility of the amorphous phase.

Introduction

The phenomenon of isomorphism between vinylidene fluoride (VF_2) and vinyl fluoride (VF) monomeric units was first discussed in 1965.[1] The very high degree of crystallinity observed for any composition ratio in the corresponding random copolymers seems to be a strong argument in favor of cocrystallization.[1]

Isomorphism between VF_2 and VF monomeric units has also been suggested for blends of the respective homopolymers of poly(vinylidene fluoride) (PVF_2) and poly(vinyl fluoride) (PVF).[1-3] In fact, X-ray analyses of the blends revealed the presence of high crystallinity for any composition ratio and consisted only of an intense crystalline peak[1-3] in the range of Bragg spacing d between 4

†Permanent address: Dipartimento di Chimica, Università di Napoli, Naples 80134, Italy.

0024-9297/86/2219-1935$01.50/0